Macromolecules

Article

pubs.acs.org/Macromolecules

Side-Chain-Controlled Self-Assembly of Polystyrene–Polypeptide Miktoarm Star Copolymers

Susanna Junnila,[†] Nikolay Houbenov,[†] Anastasis Karatzas,[‡] Nikos Hadjichristidis,[‡,⊥] Akira Hirao,[§] Hermis Iatrou,*[,‡] and Olli Ikkala*[,†]

[†]Molecular Materials, Department of Applied Physics, Aalto University (previously Helsinki University of Technology), P.O. Box 15100, 00076 Aalto, Finland

[‡]Department of Chemistry, University of Athens, Panepistimiopolis, Zografou, 15771 Athens, Greece

[§]Polymeric and Organic Materials Department, Graduate School of Science and Engineering, Tokyo Institute of Technology, Tokyo 152-8552, Japan

Supporting Information

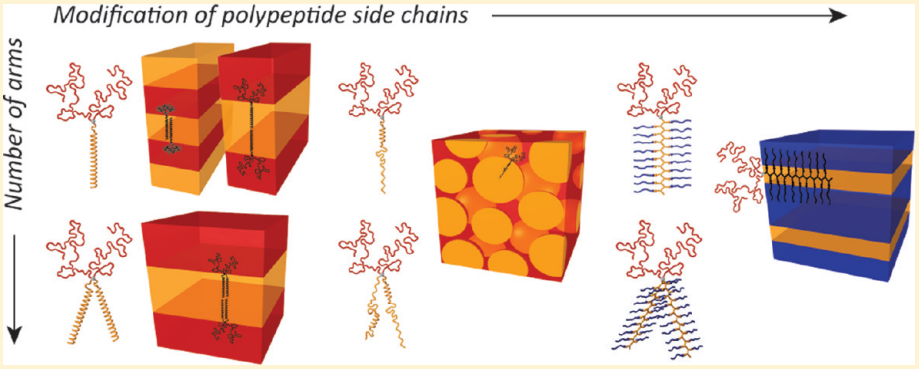

ABSTRACT: We show how the self-assembly of miktoarm star copolymers can be controlled by modifying the side chains of their polypeptide arms, using A_2B and A_2B_2 type polymer/polypeptide hybrids (macromolecular chimeras). Initially synthesized PS_2PBLL and PS_2PBLL_2 (PS, polystyrene; PBLL, poly(ε-*tert*-butyloxycarbonyl-L-lysine)) miktoarms were first deprotected to $PS_2PLLHCl$ and $PS_2PLLHCl_2$ miktoarms (PLLHCl, poly(L-lysine hydrochloride)) and then complexed ionically with sodium dodecyl sulfonate (DS) to give the supramolecular complexes $PS_2PLL(DS)$ and $PS_2(PLL(DS))_2$. The solid-state self-assemblies of these six miktoarm systems were studied by transmission electron microscopy (TEM), Fourier transform infrared spectroscopy (FTIR), and small- and wide-angle X-ray scattering (SAXS, WAXS). The side chains of the polypeptide arms were observed to have a large effect on the solubility, polypeptide conformation, and self-assembly of the miktoarms. Three main categories were observed: (i) lamellar self-assemblies at the block copolymer length scale with packed layers of α-helices in PS_2PBLL and PS_2PBLL_2; (ii) charge-clustered polypeptide micelles with less-defined conformations in a nonordered lattice within a PS matrix in $PS_2PLLHCl$ and $PS_2PLLHCl_2$; (iii) lamellar polypeptide–surfactant self-assemblies with β-sheet conformation in $PS_2PLL(DS)$ and $PS_2(PLL(DS))_2$ which dominate over the formation of block copolymer scale structures. Differences between the 3- and 4-arm systems illustrate how packing frustration between the coil-like PS arms and rigid polypeptide conformations can be relieved by the right number of arms, leading to differences in the extent of order.

INTRODUCTION

Nonlinear block copolymer architectures such as graft copolymers, star block copolymers, miktoarm star copolymers, and more complex architectures, including H-shaped and cyclic block copolymers, have recently gained much attention.[1−7] In addition to the total degree of polymerization (N), relative sizes of the blocks (f_i), and the interaction parameters (χ_{ij}) between the different monomer units, the molecular architecture also plays a significant role.

Miktoarm star copolymers are chemically asymmetric star-shaped polymers in which all blocks originate from a single branching point. In binary A_mB_n miktoarm systems composed of m blocks of polymer A and n blocks of polymer B, the minimization of interfacial tension and stretching free energy of the arms results in shifted phase boundaries compared to AB diblock copolymers.[8−10] This means that different linear and miktoarm architectures with the same volume fractions of A and B can present dissimilar self-assembled structures. The A_2B type miktoarm star copolymers are often referred to as "Y-shaped" block copolymers and can also be considered as the simplest graft copolymers.[11,12] Lamellar, cylindrical, and bicontinuous cubic morphologies have been observed for this

Received: December 20, 2011
Revised: February 22, 2012
Published: March 7, 2012

architecture.[8,13,10] At large volume fractions of B, the two A arms are forced to the concave side of the interface, leading to disordered wormlike micelles[13] and spheres.[14] For A_2B_2 miktoarm star copolymers, classical block copolymer phases including lamellar, cylindrical, and spherical morphologies have been reported.[15] Interestingly, the architecturally symmetric A_nB_n systems, in general, show larger lamellar periodicities than the corresponding diblock copolymers due to chain crowding near the junction point, which leads to an increase in chain stretching.[16,17] This effect disappears with increasing arm length.[15]

Incorporation of rigid-rod-like blocks in block copolymers increases conformational asymmetry and introduces new interactions between the anisotropic rods, leading to self-assembly behavior different from all-coil block copolymers.[18] Polypeptide blocks which adopt the α-helical conformation have been extensively used as rigid rods in linear block copolymers[19] and have recently been employed in A_2B,[20] AB_2,[21] and ABC[22,23] miktoarm systems. In the solid state, the packing of the α-helical rods typically leads to lamellar self-assemblies regardless of the volume fractions of the components.[24−26] The α-helices are not necessarily ideal, fully extended rods,[27] as their folding has been observed to depend on the length of the blocks,[24] the exact chemical nature of these blocks,[24,28] and the hydrogen-bonding capability of the casting solvent.[29]

Supramolecular interactions, particularly complexation with surfactants, have been widely used to create new self-assembled materials from block copolymers[30,31] and homopolypeptides.[32−34] Moreover, miktoarm star copolymer complexes with oppositely charged homopolymers[35] and surfactants[36] have also been studied. In addition, intramolecular association of different arms has been employed to construct pH-responsive supramolecular self-assemblies.[37,38]

Our hypothesis is that the steric packing constraints, imposed by the miktoarm architecture, together with the polypeptide conformation and possible additional supramolecular interactions, will allow tunable self-assemblies if we learn to properly control the extent of frustration. This has encouraged us to continue our studies of ABC miktoarm chimera with one polypeptide and two coil-like arms[23] with a series of A_2B and A_2B_2 type miktoarm chimeras with two polystyrene and one or two polypeptide arms. The conformation and mutual interactions of the polypeptide blocks have been modified by electrostatics and complexation with surfactants, by using poly(L-lysine) chains with *N-tert*-butyloxycarbonyl (Boc) protecting groups, their deprotected hydrochloride salt forms, and supramolecular complexes of the latter with low molecular weight surfactant. We have studied the self-assemblies by transmission electron microscopy (TEM), Fourier transform infrared spectroscopy (FTIR), and small- and wide-angle X-ray scattering (SAXS, WAXS).

EXPERIMENTAL SECTION

Synthesis. The synthesis of PS_2PBLL and PS_2PBLL_2 miktoarms has been reported previously.[39] This includes the preparation of in-chain mono- and diamino-functionalized polymers, abbreviated as PS-NH_2-PS and PS-$(NH_2)_2$-PS, by anionic polymerization high-vacuum techniques and appropriate linking chemistry. After this, the amino groups are used for the ring-opening polymerization of *ε-tert*-butyloxycarbonyl-L-lysine *N*-carboxyanhydride. $PS_2PLLHCl$ and $PS_2PLLHCl_2$ miktoarms were prepared by deprotecting the corresponding PBLL miktoarms by dissolving the polymers in dichloromethane (CH_2Cl_2, about 20% w/v) and adding an equal volume of trifluoroacetic acid (TFA) at room temperature. The solution was stirred for 2 h, after which the solvents (TFA and CH_2Cl_2) were removed by distillation in vacuum. Depending on the solubility of the final polymers, the solid polymers were dissolved or suspended in water and purified by dialysis in Milli-Q water to remove low-molecular-weight species from deprotection. Completion of the deprotection was verified by NMR spectroscopy in DMSO-d_6.[40] The molecular characteristics of the miktoarms are collected in Table 1, and the synthesis and the molecular structures are shown in Scheme 1.

Table 1. Molecular Characteristics of the Miktoarm Star Copolymers

miktoarm	$M_n \times 10^{-3}$ (g/mol)	PS−peptide composition (wt %)	M_w/M_n[a]
PS_2PBLL	31.5[a]	60.5−39.5[b]	1.02
PS_2PBLL_2	41.2[a]	48.9−51.1[b]	1.21
$PS_2PLLHCl$	28.0[c]	68.0−32.0[c]	
$PS_2PLLHCl_2$	35.3[c]	57.0−43.0[c]	
$PS_2PLL(DS)$	39.7[c]	48.0−52.0[c]	
$PS_2(PLL(DS))_2$	55.1[c]	36.6−63.4[c]	

[a]By SEC-TALLS in DMF (0.1 N LiBr) at 60 °C.[39] [b]By UV−vis spectrometry.[39] [c]Calculated based on PS_2PBLL and PS_2PBLL_2 M_n and nominal compositions.

Sample Preparation and Complexation. Bulk samples of the PS_2PBLL and PS_2PBLL_2 miktoarms were prepared by dissolving each as 1 wt % solution in chloroform ($CHCl_3$, Sigma-Aldrich, ≥99.0%) and allowing slow evaporation of the solvent over the course of ∼2 weeks, followed by drying under vacuum ($p < 10^{-2}$ mbar). $PS_2PLLHCl$ and $PS_2PLLHCl_2$ miktoarms were dissolved as 1 wt % solutions in ultrapure Milli-Q water containing 11 and 6 wt % of tetrahydrofuran (THF, Sigma-Aldrich, ≥99.9%), respectively, and the solvent mixture was slowly evaporated over the course of ∼2 weeks, followed by drying under vacuum. $PS_2PLL(DS)$ and $PS_2(PLL(DS))_2$ supramolecular complexes were prepared by mixing solutions of the $PS_2PLLHCl$ and $PS_2PLLHCl_2$ miktoarms, respectively, in 1:1 molar ratio with sodium 1-dodecanesulfonate (SDS, Aldrich, ≥99%) which was dissolved as 0.9 wt % solution in water containing 11 wt % of THF. In both cases, the combination of the constituents immediately resulted in a white precipitate. The precipitates were washed with Milli-Q water, collected, allowed to dry in air, and vacuumed.

TEM Characterization. Bulk samples were cut to 70 nm sections at −40 °C using a Leica EM UC7 Ultramicrotome and a 35° Diatome diamond knife, transferred to Quantifoil R3.5/1 holey carbon support film grids, and stained at room temperature by exposing the grids to ruthenium tetroxide (RuO_4) vapors for 1 min. The structures of PS_2PBLL, PS_2PBLL_2, $PS_2PLLHCl$, and $PS_2PLLHCl_2$ were imaged in bright-field mode with a FEI Tecnai 12 transmission electron microscope operating at an accelerating voltage of 80 kV and recorded with a Gatan UltraScan 1000 CCD camera. Small-scale structures of $PS_2PLL(DS)$ and $PS_2(PLL(DS))_2$ were imaged in bright-field mode with a JEOL JEM-3200FSC field emission transmission electron microscope operating at an accelerating voltage of 100 kV and recorded with a Gatan Ultrascan 4000 CCD camera.

SAXS and WAXS Measurements. SAXS and WAXS measurements were performed with a rotating anode Bruker Microstar microfocus X-ray source (Cu Kα radiation, λ = 1.54 Å) with two beamlines. The SAXS beam is equipped with Montel parallel optics and further collimated with four sets of JJ X-ray four-blade slits, resulting in a beam area of approximately 1 mm × 1 mm at the sample position. The scattering intensities were measured using a Bruker AXS HI-STAR 2D area detector at a sample-to-detector distance of 159 cm. The WAXS beam is equipped with Montel focusing optics, resulting in a beam area of approximately 0.8 mm × 0.8 mm at the sample position. The scattering intensities were measured with a Bruker AXS Vantec 2D area detector at a sample-to-detector distance of 10 cm. For the measurements, nonoriented bulk samples were sealed between Mylar films. Diffraction data were integrated over the whole detector

Scheme 1. Synthetic Strategy and Molecular Structures of the Synthesized and Complexed Miktoarm Star Copolymers

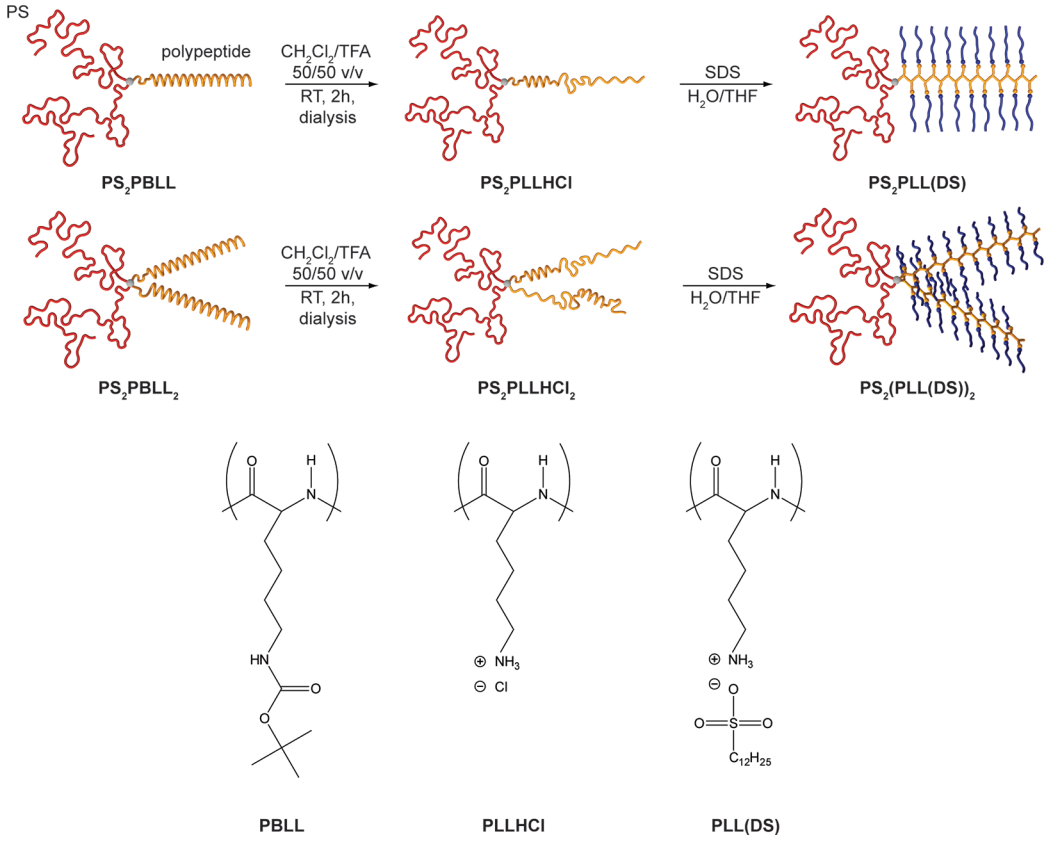

area. Background was measured separately and reduced from the spectra. The magnitude of the scattering vector is given by $q = (4\pi/\lambda) \sin \theta$, where 2θ is the scattering angle. Positions of reflections have been obtained by fitting Gaussian peaks together with an appropriate background to data that has not been Lorentz corrected.

FTIR Measurements. Dry samples were mixed with KBr and pressed into pellets. Transmission spectra were recorded with a Nicolet 380 FT-IR spectrometer. 64 spectra were averaged with 2 cm^{-1} resolution.

RESULTS AND DISCUSSION

Bulk samples of the PS_2PBLL and PS_2PBLL_2 miktoarms were prepared by slow evaporation from $CHCl_3$ with the objective of achieving equilibrium or near-equilibrium morphologies. The samples were not additionally thermally annealed since elevated temperatures have been shown to lead to partial thermal deprotection of the Boc groups of PBLL.[23] Similarly, the $PS_2PLLHCl$ and $PS_2PLLHCl_2$ miktoarms were slowly evaporated from H_2O/THF solvent mixtures. In the preparation of the supramolecular complexes, the mixing of the constituents resulted in a white precipitate which was collected and dried. Complex formation was verified by elemental analysis (see Supporting Information) which showed that 95−101% of the PLL repeating units were complexed with DS surfactants. Therefore, the complexes are denoted as $PS_2PLL(DS)$ and $PS_2(PLL(DS))_2$ according to the nominal compositions. Our aim was to use the surfactants to force the polypeptide backbone into the β-sheet conformation, which could not be achieved by other means in this study. Therefore, the precipitated complexes were studied without further treatments, knowing that organic solvent treatment may completely change the conformation of the polypeptide as well as the resulting self-assembly.[34,41]

The solid-state morphologies of the miktoarms were visualized with TEM (Figure 1). The miktoarms PS_2PBLL and PS_2PBLL_2 with protected L-lysine arms form lamellar self-assemblies which are revealed upon staining the PS blocks with RuO_4 (i.e., PS appears dark in the images). However, the self-assemblies of the 3- and 4-arm systems are not identical, as both (i) the long-range order and (ii) the lamellar periodicity differ. PS_2PBLL_2 is evidently better organized with a higher overall order and a lamellar periodicity of 13−17 nm. This indicates that there is no excessive steric frustration of the 4-arm chimera to limit a space-filling lamellar assembly. By contrast, PS_2PBLL only shows limited lamellar stacks with no apparent order observed between them. The predominant lamellar periodicity is 21−26 nm (Figure 1a). However, also lamellar stacks with a smaller periodicity of 12−16 nm are observed (additional TEM micrographs shown in the Supporting Information). This suggests higher packing frustration in the 3-arm chimera, still having propensity for the lamellar assembly.

In the $PS_2PLLHCl$ and $PS_2PLLHCl_2$ stars containing hydrochloric acid salts, TEM reveals micelles where the PLLHCl cores are surrounded by PS chains (Figure 1c,d). In both cases, the diameter of the micelles is 17−25 nm according to TEM micrographs. Similar morphologies have been previously observed in block copolymer ionomers due to charge clustering, the aggregation number of the micelles ranging from tens to several hundreds depending on the counterion and block copolymer composition.[42] Finally, in the supramolecular complexes $PS_2PLL(DS)$ and $PS_2(PLL(DS))_2$, lamellar self-assemblies with periodicities of ca. 4 nm are found (Figure 1e,f). These lamellae are composed of the alternating polypeptide and surfactant layers of the PLL(DS) arms. As the complex

dx.doi.org/10.1021/ma202747h | Macromolecules 2012, 45, 2850−2856

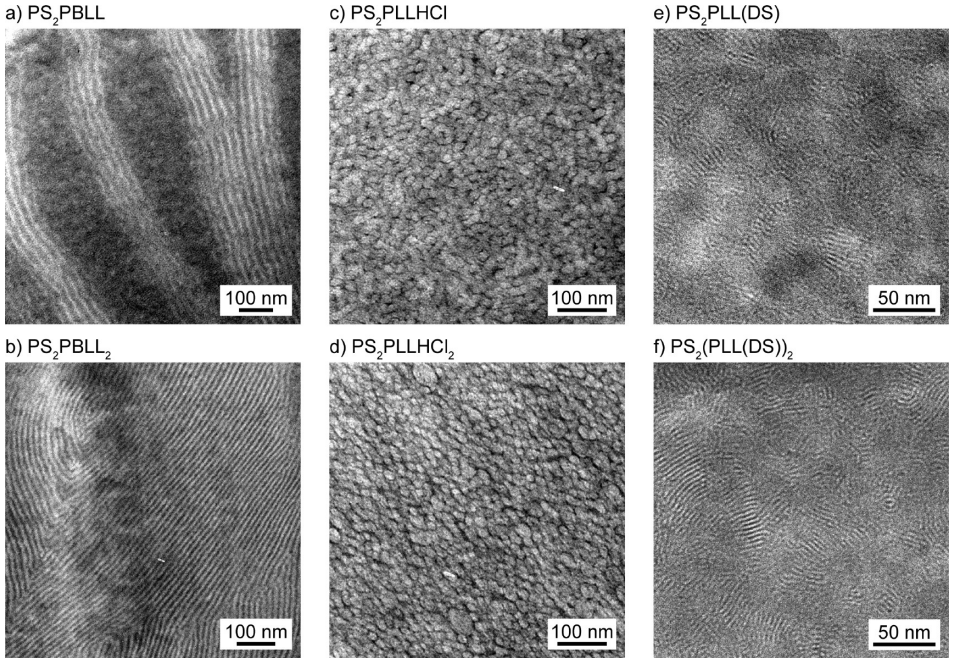

Figure 1. TEM micrographs of the miktoarm bulk samples, stained with RuO_4 (PS dark). Note the different scale in the organization of (a–d) compared to (e, f). Additional TEM micrographs of PS_2PBLL are shown in the Supporting Information.

lamellar areas are rather small and randomly oriented, the PS chains that surround the lamellae do not form any well-ordered phases on the block copolymer length scale; therefore, TEM does not reveal any clear structures on the block copolymer scale.

SAXS (Figure 2) was used to verify the block copolymer scale structures observed in TEM and to extract more exact

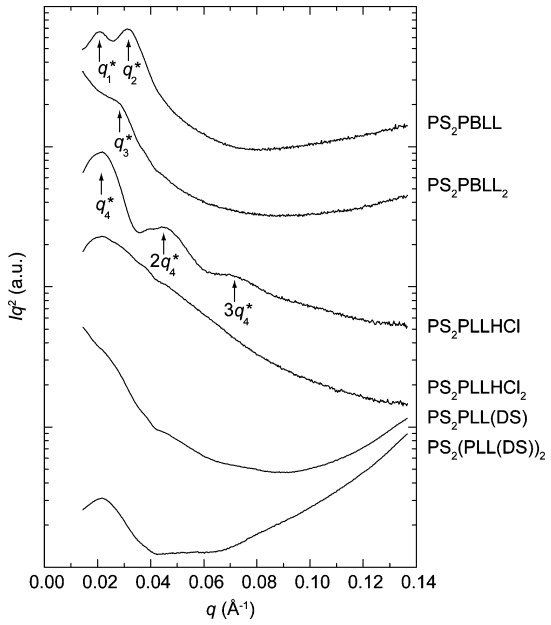

Figure 2. SAXS curves of the miktoarm star copolymers.

information about the structural sizes. For PS_2PBLL, two reflections are observed at $q_1^* = 0.020$ Å^{-1} and $q_2^* = 0.032$ Å^{-1}, corresponding to 31 and 20 nm structures, respectively. These reflections verify the coexistence of two different lamellar long periods, as observed in TEM (Figure 1a and Figure S1). PS_2PBLL_2 shows a single shoulder at $q_3^* = 0.028$ Å^{-1}, corresponding to a lamellar long period of 22 nm. A very similar scattering curve was observed previously in the lamellar self-assembly of an ABC miktoarm star chimera with a single polypeptide arm.[23] The micellar-forming $PS_2PLLHCl$ has three broad reflections at $q_4^* = 0.019$ Å^{-1}, $2q_4^*$, and $3q_4^*$ which correspond to a structural size of 33 nm. This reflects the average distance of the polypeptide micelles in the PS matrix, although they do not form a well-defined lattice. $PS_2PLLHCl_2$ shows a broad reflection at low q range, probably due to a similar structure as in $PS_2PLLHCl$, as suggested by TEM. It is hard to extract a structural size for this sample in a meaningful way from the SAXS data, as scattering intensity remains relatively high toward larger q values. The absence of well-defined micelle-to-micelle reflections could be an indication of higher polydispersity in the micellar size of $PS_2PLLHCl_2$. For the supramolecular complexes, no reflections are expected in SAXS, as no block copolymer scale organization was observed in TEM. However, $PS_2(PLL(DS))_2$ shows a broad reflection at 0.021 Å^{-1}, which corresponds to a structural size of 30 nm. This reflection is tentatively assigned to the average distance of neighboring polypeptide–surfactant domains.

The conformation of the polypeptide arms was studied by FTIR (Figure 3). PS_2PBLL and PS_2PBLL_2 show a sharp amide I band at 1651 cm^{-1}, originating mainly from the C=O stretching of peptide bonds participating in α-helical conformation.[43] Additionally, the Boc protecting groups give rise to the two broad bands at 1714 and 1686 cm^{-1}. The amide II region at 1560–1520 cm^{-1} shows multiple overlapping bands and is not therefore used to interpret the polypeptide conformation. The spectra of $PS_2PLLHCl$ and $PS_2PLLHCl_2$ display a number of different amide I bands at 1652 and 1618 cm^{-1} for $PS_2PLLHCl$ and at 1682, 1653, and 1626 cm^{-1} for $PS_2PLLHCl_2$. These multiple bands are evidence of a mixture of conformations for the PLLHCl arms, including α-helices and antiparallel β-sheets for $PS_2PLLHCl$, and, in addition, turns[44] observed near 1680 cm^{-1} for $PS_2PLLHCl_2$. Therefore, the

dx.doi.org/10.1021/ma202747h | Macromolecules 2012, 45, 2850–2856

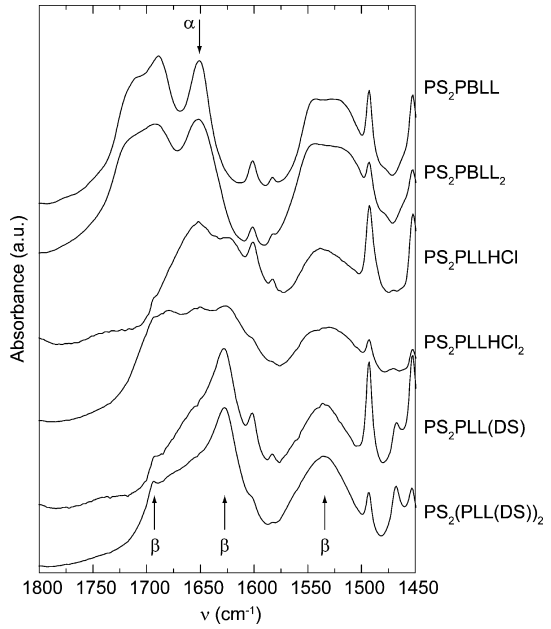

Figure 3. FTIR spectra of the miktoarm star copolymers.

conformation is not well-defined in these miktoarms. Also surfactant complexation of the polypeptide arms results in dramatic conformational changes: both $PS_2PLL(DS)$ and $PS_2(PLL(DS))_2$ show amide I bands at 1693−1692 and 1628 cm^{-1} corresponding to antiparallel β-sheets with small amounts of α-helical or random coil conformations at ∼1660 cm^{-1}. The amide II band can now also be used and its location at 1535 cm^{-1} supports this interpretation.

The differences in the morphologies and conformations of the miktoarms are also evident in WAXS (Figure 4). Packing of

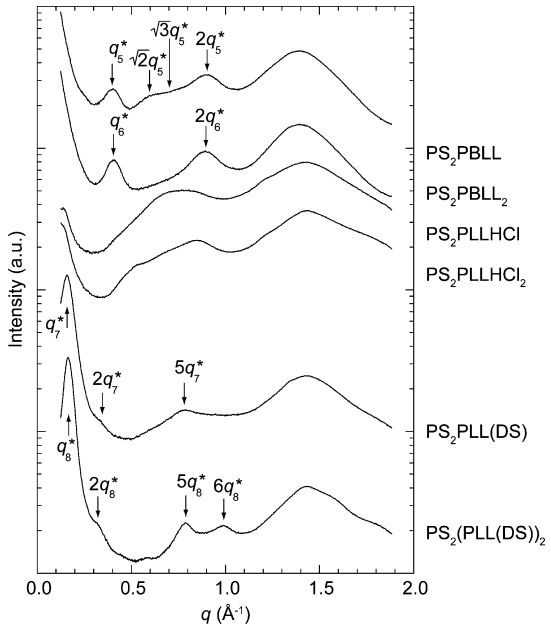

Figure 4. WAXS curves of the miktoarm star copolymers.

the relatively rod-like α-helices is observed for PS_2PBLL at q_5^* = 0.40 $Å^{-1}$, $\sqrt{2}q_5^*$, $\sqrt{3}q_5^*$, and $2q_5^*$ (see Supporting Information for detailed fitting) which strongly implies coexistence of both hexagonal and tetragonal local packing. The helix-to-helix distance is, based on the value of q_5^*, 1.6 and 1.8 nm in the tetragonal and hexagonal arrangements, respectively. Previously, hexagonal packing of α-helices have been reported in several polymer/polypeptide chimeras.[24,45,25] In our case, however, the added interfacial frustration of the miktoarm architecture might lead to a different kind of packing from the one typically favored by linear chimeras. For PS_2PBLL_2, distinct WAXS reflections q_6^* = 0.40 $Å^{-1}$ and $2q_6^*$ are observed, but the absence of $\sqrt{2}q_6^*$ or $\sqrt{3}q_6^*$ reflections prevents unambiguous assignment of the helical packing geometry.

In the direction perpendicular to the lamellae, the helices can either (i) stack to form bilayers, (ii) interdigitate, or (iii) fold back and forth as kinked rods.[21,24] Based on the molecular weights of the polypeptide arms and the well-known geometry of the α-helix, the length of a single ideal α-helical arm, L_{helix}, is 8.2 nm for the present PS_2PBLL and 6.9 nm for PS_2PBLL_2. Bilayer stacking of helices will then require a polypeptide layer thickness, $d_{peptide}$, of up to $\sim 2L_{helix}$ while interdigitation leads to $d_{peptide}$ which is $\sim L_{helix}$. Tilting can, in both cases, reduce the thickness of the polypeptide layer. Folding of the helices back and forth, on the other hand, always leads to $d_{peptide} < L_{helix}$.[24] Considering the overall periodicity as observed in SAXS, the weight fractions of the blocks, and the specific volumes of PBLL and PS, conclusions can be drawn from the probable packing of the PBLL α-helices (Table 2). The relatively small molecular weights[24] and casting from a weakly hydrogen-bonding solvent[29] support the formation of nearly ideal α-helices in the present study. Therefore, comparing $d_{peptide}$ to L_{helix} should give a direct measure of the packing of the helices. For the PS_2PBLL lamellar self-assembly with 20 nm periodicity, the value of 1.06 implies very perfect interdigitation of the helices in an approximately perpendicular direction to the block copolymer scale lamellae. Interdigitation has also previously been observed in a miktoarm chimera with two different coil-like arms and one polypeptide arm.[23] On the other hand, the larger PS_2PBLL periodicity of 31 nm cannot be explained by folding or tilting, since they would both reduce the thickness. The value of 1.64 for the relation of $d_{peptide}$ and L_{helix} must therefore represent a stacked bilayer of α-helices. A very similar figure is obtained for PS_2PBLL_2, also suggested to represent a stacked bilayer configuration. This is reasonable, as the addition of a second polypeptide arm should drive the balance between the interdigitated and stacked configurations, both observed in the 3-arm system, toward the stacked bilayer configuration for the 4-arm system. Previously, stacked bilayers have been reported for miktoarms with one coil-like arm and two polypeptide arms, regardless of the weight fractions of the components.[21] The structures are schematically illustrated in Figure 5.

For $PS_2PLLHCl$ and $PS_2PLLHCl_2$, WAXS (Figure 4) does not show distinct small-scale structures other than broad correlation reflections. This is not surprising, taking into account the mixed conformations of the PLLHCl arms discussed above. On the other hand, the polypeptide−surfactant organization of $PS_2PLL(DS)$ and $PS_2(PLL(DS))_2$ observed in TEM (Figure 1e,f) is clearly confirmed by WAXS. For $PS_2PLL(DS)$, reflections q_7^* = 0.16 $Å^{-1}$, $2q_7^*$, and $5q_7^*$ are observed, corresponding to a lamellar periodicity of 3.9 nm. This fits well with the thickness of a single PLL β-sheet (1.5 nm) surrounded on each side by C_{12} chains and also with previous reports on polymer−surfactant[46,47] and polypeptide−surfactant complexes[32,40] with C_{12} surfactants. No evidence of crystallization

dx.doi.org/10.1021/ma202747h | Macromolecules 2012, 45, 2850−2856

Table 2. Helix Packing Geometry in the PS_2PBLL and PS_2PBLL_2 Miktoarms

miktoarm	d_{SAXS}[a] (nm)	$d_{peptide}$[b] (nm)	d_{PS}[c] (nm)	L_{helix}[d] (nm)	$d_{peptide}/L_{helix}$	helix packing geometry
PS_2PBLL	31	13.4	17.6	8.2	1.64	bilayer
	20	8.7	11.3	8.2	1.06	interdigitation
PS_2PBLL_2	22	12.1	9.9	6.9	1.75	bilayer

[a] d_{SAXS}: lamellar long period from SAXS. [b] Thickness of polypeptide layer $d_{peptide} = d_{SAXS}(1 + w_{PS}\nu_{PS}/w_{PBLL}\nu_{PBLL})^{-1}$ where w is mass fraction and ν specific volume, $\nu_{PS} = 0.95$ and $\nu_{PBLL} = 1.11$ cm^3/g. [c] Thickness of PS layer $d_{PS} = d_{SAXS} - d_{peptide}$. [d] Length of an ideal α-helical PBLL arm, $L_{helix} = N_{PBLL} \times 0.15$ nm/n, where N_{PBLL} = degree of polymerization of PBLL and n = number of PBLL arms.

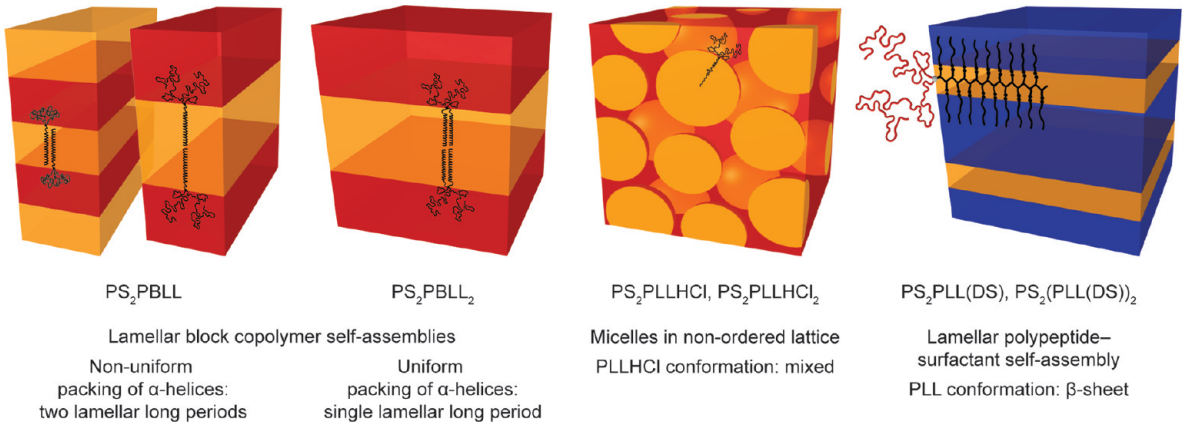

Figure 5. Schematic illustration of the packing of the miktoarm molecules in bulk (red, PS; yellow, polypeptide; blue, surfactant).

of the C_{12} chains[41] can be found in the WAXS curve, and hence they are expected to take up slightly less space than in the all-trans conformation (1.5 nm). The broad reflection located at 1.39−1.44 Å^{-1} in all of the miktoarms reflects average distances between the amorphous segments of the polymers[21] and is here overlapped with the amorphous halo from the surfactant tails. Slightly more intense reflections are observed for $PS_2(PLL(DS))_2$ at $q_8^* = 0.16$ Å^{-1}, $2q_8^*$, $5q_8^*$, and $6q_8^*$ which imply that the 4-arm system is structurally identical but to some extent better organized. The multiple reflections in WAXS demonstrate well-ordered packing of the PLL(DS) complex arms which overrides the block copolymer scale organization. On the other hand, the existence of the PS arms brings frustration into the systems and effectively limits the size of the PLL(DS) domains, as observed in TEM (Figure 1e,f). The fact that $PS_2(PLL(DS))_2$ is observed to form slightly larger self-assembled domains in TEM illustrates how the number of competing arms needs to be balanced to relieve interfacial frustration.

CONCLUSIONS

We have shown how modification of the polypeptide arms can be used to control the self-assemblies of A_2B and A_2B_2 type miktoarm star copolymer chimeras. The side chains of the polypeptide arms influence not only solubility but also conformation and, therefore, self-assembly of the systems in the solid state due to modified packing frustration. In PS_2PBLL and PS_2PBLL_2 miktoarms, the α-helical polypeptide conformation promotes lamellar self-assemblies. The frustration between the rod-like PBLL and the coil-like PS arms leads to a suppressed ability of PS_2PBLL to form an overall, space-filling lamellar order, and structures with two different packing mechanisms of the α-helical arms are observed. In PS_2PBLL_2, the frustration is better balanced, and a uniform lamellar self-assembly with bilayer stacking of the α-helices is observed. In the miktoarms with PLLHCl salts, polyelectrolytic charge clustering leads to polypeptide micelles which show relatively random polypeptide conformations and are located in a nonordered lattice within a PS matrix. Ionic complexation of the polypeptide arms with DS leads to particularly pronounced small-scale ordering of the polypeptide−surfactant complex arms which dominates over the formation of block copolymer scale structures. These findings pave the way for learning to balance frustration, supramolecular concepts, and tunable properties in new polymer materials.

ASSOCIATED CONTENT

Supporting Information

Elemental analysis of $PS_2PLL(DS)$ and $PS_2(PLL(DS))_2$, additional TEM micrographs of PS_2PBLL, and fitting of the WAXS curve of PS_2PBLL. This material is available free of charge via the Internet at http://pubs.acs.org.

AUTHOR INFORMATION

Corresponding Author

*E-mail: olli.ikkala@aalto.fi (O.I.), iatrou@chem.uoa.gr (H.I.).

Present Address

[⊥]4700 King Abdullah University of Science and Technology, Thuwal 23955-6900, Kingdom of Saudi Arabia.

Notes

The authors declare no competing financial interest.

ACKNOWLEDGMENTS

This work made use of the Aalto University Nanomicroscopy Center (Aalto-NMC) premises. Dr. Jani Seitsonen is thanked for the TEM imaging of the surfactant-scale structures and Panu Hiekkataipale for the assistance and discussions regarding SAXS/WAXS experiments. The Academy of Finland is gratefully acknowledged for financial support.

REFERENCES

(1) Pitsikalis, M.; Pispas, S.; Mays, J. W.; Hadjichristidis, N. *Adv. Polym. Sci.* **1998**, *135*, 1−137.
(2) Ishizu, K.; Uchida, S. *Prog. Polym. Sci.* **1999**, *24*, 1439−1480.
(3) Tezuka, Y.; Oike, H. *Prog. Polym. Sci.* **2002**, *27*, 1069−1122.
(4) Ge, Z. S.; Liu, S. Y. *Macromol. Rapid Commun.* **2009**, *30*, 1523−1532.
(5) Hirao, A.; Murano, K.; Oie, T.; Uematsu, M.; Goseki, R.; Matsuo, Y. *Polym. Chem.* **2011**, *2*, 1219−1233.
(6) Read, D. J.; Auhl, D.; Das, C.; den Doelder, J.; Kapnistos, M.; Vittorias, I.; McLeish, T. C. B. *Science* **2011**, *333*, 1871−1874.
(7) Ungar, G.; Tschierske, C.; Abetz, V.; Holyst, R.; Bates, M. A.; Liu, F.; Prehm, M.; Kieffer, R.; Zeng, X. B.; Walker, M.; Glettner, B.; Zywocinski, A. *Adv. Funct. Mater.* **2011**, *21*, 1296−1323.
(8) Hadjichristidis, N.; Iatrou, H.; Behal, S. K.; Chludzinski, J. J.; Disko, M. M.; Garner, R. T.; Liang, K. S.; Lohse, D. J.; Milner, S. T. *Macromolecules* **1993**, *26*, 5812−5815.
(9) Milner, S. T. *Macromolecules* **1994**, *27*, 2333−2335.
(10) Tselikas, Y.; Iatrou, H.; Hadjichristidis, N.; Liang, K. S.; Mohanty, K.; Lohse, D. J. *J. Chem. Phys.* **1996**, *105*, 2456−2462.
(11) Pennisi, R. W.; Fetters, L. J. *Macromolecules* **1988**, *21*, 1094−1099.
(12) Mays, J. W. *Polym. Bull.* **1990**, *23*, 247−250.
(13) Pochan, D. J.; Gido, S. P.; Pispas, S.; Mays, J. W.; Ryan, A. J.; Fairclough, J. P. A; Hamley, I. W.; Terrill, N. J. *Macromolecules* **1996**, *29*, 5091−5098.
(14) Mavroudis, A.; Avgeropoulos, A.; Hadjichristidis, N.; Thomas, E. L.; Lohse, D. J. *Chem. Mater.* **2003**, *15*, 1976−1983.
(15) Beyer, F. L.; Gido, S. P.; Uhrig, D.; Mays, J. W.; Tan, N. B.; Trevino, S. F. *J. Polym. Sci., Part B: Polym. Phys.* **1999**, *37*, 3392−3400.
(16) Turner, C. M.; Sheller, N. B.; Foster, M. D.; Lee, B.; Corona-Galvan, S.; Quirk, R. P.; Annis, B.; Lin, J. S. *Macromolecules* **1998**, *31*, 4372−4375.
(17) Zhu, Y. Q.; Gido, S. P.; Moshakou, M.; Iatrou, H.; Hadjichristidis, N.; Park, S.; Chang, T. *Macromolecules* **2003**, *36*, 5719−5724.
(18) Olsen, B. D.; Segalman, R. A. *Mater. Sci. Eng., R* **2008**, *62*, 37−66.
(19) Gallot, B. *Prog. Polym. Sci.* **1996**, *21*, 1035−1088.
(20) Sun, J.; Chen, X. S.; Guo, J. S.; Shi, Q.; Xie, Z. G.; Jing, X. B. *Polymer* **2009**, *50*, 455−461.
(21) Babin, J.; Taton, D.; Brinkmann, M.; Lecommandoux, S. *Macromolecules* **2008**, *41*, 1384−1392.
(22) Gitsas, A.; Floudas, G.; Mondeshki, M.; Lieberwirth, I.; Spiess, H. W.; Iatrou, H.; Hadjichristidis, N.; Hirao, A. *Macromolecules* **2010**, *43*, 1874−1881.
(23) Junnila, S.; Houbenov, N.; Hanski, S.; Iatrou, H.; Hirao, A.; Hadjichristidis, N.; Ikkala, O. *Macromolecules* **2010**, *43*, 9071−9076.
(24) Douy, A.; Gallot, B. *Polymer* **1982**, *23*, 1039−1044.
(25) Schlaad, H.; Kukula, H.; Smarsly, B.; Antonietti, M.; Pakula, T. *Polymer* **2002**, *43*, 5321−5328.
(26) Schlaad, H.; Smarsly, B.; Losik, M. *Macromolecules* **2004**, *37*, 2210−2214.
(27) Papadopoulos, P.; Floudas, G.; Klok, H. A.; Schnell, I.; Pakula, T. *Biomacromolecules* **2004**, *5*, 81−91.
(28) Losik, M.; Kubowicz, S.; Smarsly, B.; Schlaad, H. *Eur. Phys. J. E* **2004**, *15*, 407−411.
(29) Schlaad, H.; Smarsly, B.; Below, I. *Macromolecules* **2006**, *39*, 4631−4632.
(30) Ikkala, O.; ten Brinke, G. *Chem. Commun.* **2004**, *19*, 2131−2137.
(31) Hammond, M. R.; Mezzenga, R. *Soft Matter* **2008**, *4*, 952−961.
(32) Ponomarenko, E. A.; Tirrell, D. A.; MacKnight, W. J. *Macromolecules* **1996**, *29*, 8751−8758.
(33) Canilho, N.; Scholl, M.; Klok, H. A.; Mezzenga, R. *Macromolecules* **2007**, *40*, 8374−8383.
(34) Hanski, S.; Junnila, S.; Almasy, L.; Ruokolainen, J.; Ikkala, O. *Macromolecules* **2008**, *41*, 866−872.
(35) Li, J.; He, W. D.; He, N.; Han, S. C.; Sun, X. L.; Li, L. Y.; Zhang, B. Y. *J. Polym. Sci., Polym. Chem.* **2009**, *47*, 1450−1462.
(36) Hammond, M. R.; Li, C. X.; Tsitsilianis, C.; Mezzenga, R. *Soft Matter* **2009**, *5*, 2371−2377.
(37) Liu, H.; Li, C. H.; Liu, H. W.; Liu, S. Y. *Langmuir* **2009**, *25*, 4724−4734.
(38) Iatridi, Z.; Tsitsilianis, C. *Chem. Commun.* **2011**, *47*, 5560−5562.
(39) Karatzas, A.; Iatrou, H.; Hadjichristidis, N.; Inoue, K.; Sugiyama, K.; Hirao, A. *Biomacromolecules* **2008**, *9*, 2072−2080.
(40) Hanski, S.; Houbenov, N.; Ruokolainen, J.; Chondronicola, D.; Iatrou, H.; Hadjichristidis, N.; Ikkala, O. *Biomacromolecules* **2006**, *7*, 3379−3384.
(41) Junnila, S.; Hanski, S.; Oakley, R. J.; Nummelin, S.; Ruokolainen, J.; Faul, C. F. J.; Ikkala, O. *Biomacromolecules* **2009**, *10*, 2787−2794.
(42) Moffitt, M.; Eisenberg, A. *Macromolecules* **1997**, *30*, 4363−4373.
(43) Lee, N. H.; Frank, C. W. *Langmuir* **2003**, *19*, 1295−1303.
(44) Krimm, S.; Bandekar, J. *Adv. Protein Chem.* **1986**, *38*, 181−364.
(45) Klok, H. A.; Langenwalter, J. F.; Lecommandoux, S. *Macromolecules* **2000**, *33*, 7819−7826.
(46) Bergström, M.; Kjellin, U. R. M.; Claesson, P. M.; Pedersen, J. S.; Nielsen, M. M. *J. Phys. Chem. B* **2002**, *106*, 11412−11419.
(47) Starodubtsev, S. G.; Laptinskaya, T. V.; Yesakova, A. S.; Khokhlov, A. R.; Shtykova, E. V.; Dembo, K. A.; Volkov, V. V. *Polymer* **2010**, *51*, 122−128.